

## DIFFUSION IN TEVATRON USING FLYING WIRE

S. Shiraishi, University of Chicago, Chicago, IL 60637, USA

R. J. Tesarek, Fermi National Accelerator Laboratory, Batavia, IL 60510, USA

### Abstract

Understanding beam loss in an accelerator is crucial to accelerator design and operation. Losses contribute to a shorter lifetime of a circulating beam, higher radiation doses to accelerator components, and backgrounds in experiments which use the beam. One source of beam loss is diffusion caused by effects such as beam scattering with residual gas in vacuum chamber, noise in the radio frequency acceleration system and power supplies, and beam-beam collisions [1]. We measure the diffusion rate in the Fermilab Tevatron using the flying wire beam profile monitor. We have developed a new technique for interpreting the flying wire data. Using this technique, we measure the proton horizontal diffusion rate for ten stores in the Tevatron during colliding beam operation.

### INTRODUCTION

Noise in the radio frequency acceleration system and power supplies, beam-gas interactions, and beam-beam scattering increase the oscillation amplitude of the beam particles. This process leads to a slow growth in the beam width and is referred to as the transverse diffusion. Measuring the beam growth rate allows us to infer the emittance growth for the stored beam. We use a flying wire beam profile monitor to measure beam width. The flying wire is a primary beam profile monitor in the Tevatron. Other instruments such as Synchrotron Light Monitor, Ionization Profile Monitors, and Microwave Schottky detectors are also available. [2]

### FLYING WIRE SYSTEM

Flying wire is a beam profile monitor in Fermilab Tevatron in which a carbon fiber of thickness  $5\mu\text{m}$  is passed through the beam and causes scattering [2, 3] (Fig. 1). Some of the scattered and secondary particles are detected by a scintillation counter located downstream. The current measured by the counter is therefore related to the beam profile. The current charges a capacitor whose voltage is recorded as a function of time. This voltage along with the wire position make a profile. The wire can move in a clockwise (CW) or counter clockwise (CCW) direction in the horizontal plane, and profiles are taken at upstream and downstream interaction points (IP) as shown in Fig. 1. A total of 72 profiles, two profiles for each of the 36 bunches, are recorded for each fly, and a flying wire measurement is taken every hour during a Tevatron store.

We study data taken during High Energy Physics (HEP) collisions for 10 selected stores from June 2008. The date,

**Beam Dynamics and Electromagnetic Fields**

**D03 - High Intensity - Incoherent Instabilities, Space Charge, Halos, Cooling**

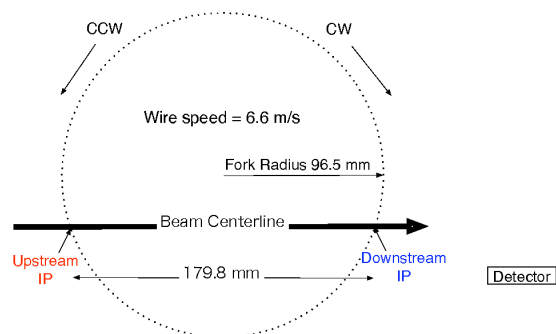


Figure 1: Schematic of flying wire viewed from the top of the flying wire can. Dots on the circle represents the path of the wire. Each dot is a location of wire at a given time. The wire is vertical into the paper in this diagram.

length, initial luminosity, and particle intensities for those stores are listed in Table 1.

Table 1: List of stores analyzed. Stores are selected from June 2008.

Date	Length [hr]	Init. Lumi. [E30]	No. of $p$ [E9]	No. of $\bar{p}$ [E9]
06.06	25.0	295.3	9755	2739
06.07	13.5	287.0	8968	3040
06.10	24.5	211.4	9905	2314
06.11	28.5	214.6	9989	1948
06.12	18.2	191.2	9798	2140
06.21	16.0	271.7	9419	2892
06.21	28.7	278.7	9525	2859
06.24	17.9	201.4	9512	1939
06.26	17.3	281.7	9346	2813
06.27	20.4	267.7	9256	2707

### CALIBRATIONS

Calibrations are performed to extract consistent information from the profiles. First, a pedestal defined as the average of 25 data points when the wire is out of the beam is subtracted from each profile.

Second, we estimate the uncertainty for each measurement as in Eq. 1,

$$\sigma(x) = \sqrt{\sigma_{ped}^2(x) + (\alpha\sqrt{A_{data}(x)})^2}, \quad (1)$$

where the first term represents electronic noise and the second term represents uncertainty from counting particles with the counter. We define  $\sigma_{ped}$  as the RMS of 25 data points when the wire is out of beam, and  $A_{data}$  is the measured amplitude. The constant  $\alpha$  is defined so that the pull distribution is centered around zero and has a unit width, where the pull is defined as  $(A_{data}(x) - A_{fit}(x))/\sigma(x)$ . A double Gaussian probability density function (PDF) is used for the fit. The constant  $\alpha$  is 0.235 and 0.355 for upstream and downstream profiles, respectively, for all 10 stores.

Third, the area under beam profile is set equal to the number of protons measured by the Fast Bunch Integrator (FBI), an instrument that measures beam current [4]. We use the same scaling for both upstream and downstream profiles and for all stores.

In addition, we calibrate two systematic effects: a difference in the acceptance ratio for upstream and downstream interactions and intensity dependent detector response. The detector subtends a larger solid angle of scattered particles from the downstream IP because the detector is closer to the downstream, resulting in a difference in acceptance ratio. Moreover, the sensitivity of the detector response depends on the beam intensity. We calibrate these effects using FBI so the area under the beam profiles is equal to the number of protons in the bunch for all intensities for both upstream and downstream profiles.

## ASYMMETRIC BEAM PROFILES

Flying wire beam profiles are asymmetric with the asymmetry depending on fly direction and IP (Fig. 2). An upstream profile has a tail on the left and downstream profile has a tail on the right for a CW fly. The location of the tail is reversed for a CCW fly. We accommodate this effect with a scattering model for the detector response described below.

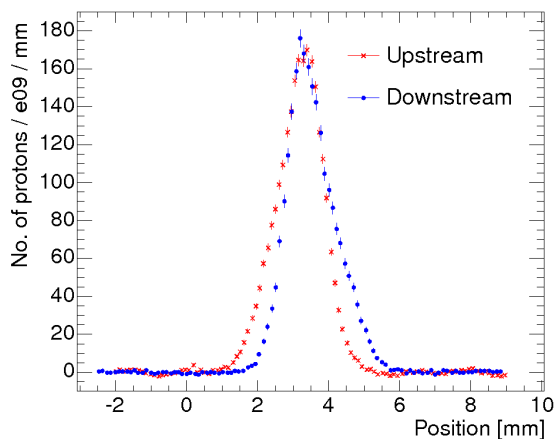


Figure 2: Flying wire data for CW fly. Upstream (red) and downstream (blue) profiles are translated and overlaid for comparison.

## SCATTERING MODEL

The observed asymmetric tail may be described using a model which allows for scattered beam particles to interact with the wire again on subsequent revolutions. When the wire hits the beam, it scatters particles into the detector. As the wire proceeds further into the beam, it scatters particles from the beam as well as residual particles from previous scattering. Figure 3 illustrates the concept of the scattering model for a square beam. According to this model, the detector response is equivalent to a square beam and a Gaussian PDF convoluted up to the point of measurement. For a real proton beam, we replace the square beam with a Gaussian beam to describe the flying wire beam profiles. The functional forms describing the detector response in

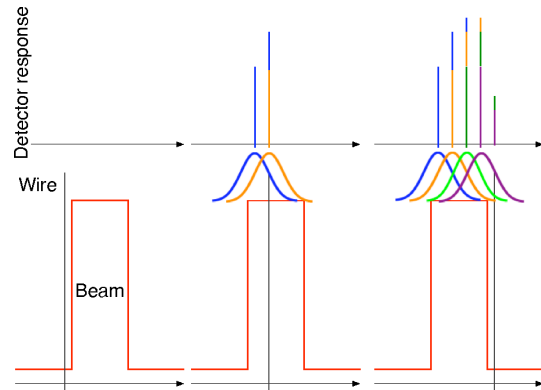


Figure 3: Illustration of the scattering model. Rectangles represent the beam, the vertical lines represent the wire, and the detector response is illustrated at the top. The Gaussian PDFs represent particles scattered from the interaction, and the horizontal axis represents position.

the scattering model are shown in Eq. 2. In this equation,  $N_P$  is the normalization which is scaled to be the beam intensity of the bunch,  $\sigma_B$  and  $\mu$  are the width and the location of the Gaussian PDF describing the beam, and  $\sigma_S$  is the width of the scattering distribution. Profiles with tails on the right are described by  $f_R(x)$  and those with tails on the left are described by  $f_L(x)$ .

$$f_R(x) = \int_{-\infty}^x \frac{N_P}{\pi \sigma_B \sigma_S} e^{-\frac{(x'-\mu)^2}{2\sigma_B^2}} e^{-\frac{(x-x')^2}{2\sigma_S^2}} dx',$$

$$f_L(x) = \int_x^{\infty} \frac{N_P}{\pi \sigma_B \sigma_S} e^{-\frac{(x'-\mu)^2}{2\sigma_B^2}} e^{-\frac{(x-x')^2}{2\sigma_S^2}} dx'. \quad (2)$$

We use the scattering model to fit the flying wire data. The free parameters in the fit are from the beam ( $N_P$ ,  $\sigma_B$ ,  $\mu$ ) and  $\sigma_S$  from the scattering. We interpret the 'beam parameters' as those associated with the unperturbed beam. We expect the scattering width ( $\sigma_S$ ) to be constant for all flies taken with the same beam energy. In addition to describing the peaks with these parameters, we also fit a linear function to accommodate the baseline. An example of a fit is shown in Fig. 4. The model describes the data well including the asymmetric tail.

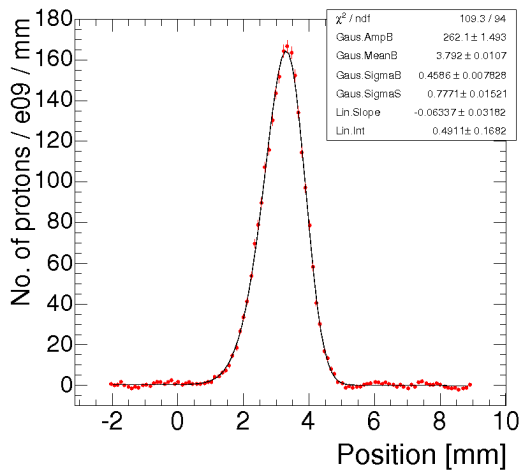


Figure 4: Typical fit to an upstream beam profile for CW fly using Eqn. 2.

## DIFFUSION RATE

Four fit parameters,  $N_P$ ,  $\sigma_B$ ,  $\mu$  and  $\sigma_S$ , describe the shape of the profile. The first three parameters describe the beam and the parameter,  $\sigma_S$ , describes the effect of the wire on the measurement. Fits to data show that  $\sigma_S$  is roughly constant (1.2% variation) for all 36 bunches and for all 10 stores as expected from our model. We use  $\sigma_B$  as beam width and study the growth rate as a function of time during HEP stores. We fit a linear function to  $\sigma_B$  as a function of time as shown in Fig. 5. The slope of the linear fit represents the beam width growth rate and is consistent for upstream and downstream profiles and all 36 bunches. The growth rates for the 10 stores are expected to be similar because we have chosen stores that are close in time. The average beam width growth rate of the 10 stores, combining upstream and downstream measurements, is  $(8.89 \pm 0.02) \times 10^{-3}$  mm/hour. Diffusion rate,

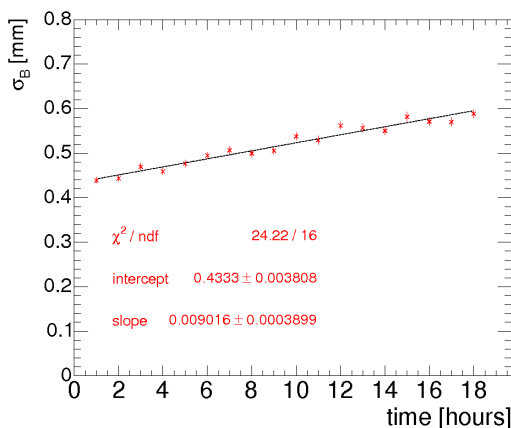


Figure 5: Beam width growth rate for a bunch in a store from upstream profiles.

defined as  $d\sigma_B^2/dt$ , is shown in Fig. 6 for the 10 stores. Each point is the average of 36 bunches. The average of the 10 stores, combining upstream and downstream measurements, is  $(8.93 \pm 0.01) \times 10^{-3}$  mm<sup>2</sup>/hour.

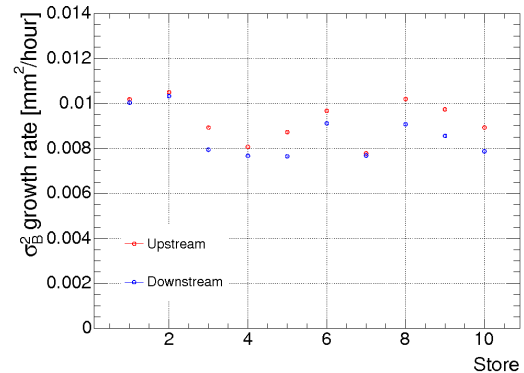


Figure 6: Diffusion rate, defined as  $d\sigma_B^2/dt$ , for 10 stores. Each point is an average of 36 bunches.

## CONCLUSION

Horizontal proton profiles measured by the flying wire in the Tevatron have been analyzed. We observe mechanical effects such as a difference in acceptance ratio between upstream and downstream profiles, intensity dependent detector response, and asymmetric beam profiles. The first two effects have been calibrated against FBI measurements. We have proposed a scattering model that could explain the asymmetric profiles, and our model is reasonably consistent with the data. Horizontal beam growth rate for the proton beam in the Tevatron during the stores is measured to be  $(8.89 \pm 0.02) \times 10^{-3}$  mm/hour for a typical store. We also measure that  $\sigma_B^2$  changes  $(8.93 \pm 0.01) \times 10^{-3}$  mm<sup>2</sup>/hour for the same stores.

## ACKNOWLEDGEMENTS

We are grateful to Y. K. Kim, D. Slimmer, M. Syphers, and J. Zagel for useful discussions and support.

## REFERENCES

- [1] M. J. Syphers, "An Analytical Approach to Understanding Tevatron Integrated Luminosity", Fermilab-FN-08020-AD, May 2007.
- [2] J. Zagel, M. Hu, A. Jansson, R. Thurman-Keup, and M. J. Yang, "Complementary Method of Transverse Emittance Measurement", BIW08, Lake Tahoe, CA, May 2008.
- [3] C. Christensen, "Flying Wire Geometry", Fermilab-Beamsdoc-765-v5, June 2005.
- [4] J. Utterback, G. Vogel, "Fast Bunch Integrator: A system for measuring bunch intensities in Fermilab main ring", ICALEPCS 95, Chicago, IL, Oct. 1995.